

Structure, stability, and electronic property of carbon-doped gold clusters $AunC$ ($n = 1-10$): A density functional theory study

Li-Li Yan, Yi-Rong Liu, Teng Huang, Shuai Jiang, Hui Wen, Yan-Bo Gai, Wei-Jun Zhang, and Wei Huang

Citation: *The Journal of Chemical Physics* **139**, 244312 (2013); doi: 10.1063/1.4852179

View online: <http://dx.doi.org/10.1063/1.4852179>

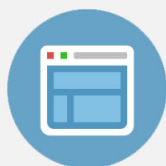
View Table of Contents: <http://scitation.aip.org/content/aip/journal/jcp/139/24?ver=pdfcov>

Published by the [AIP Publishing](#)



Re-register for Table of Content Alerts

Create a profile.



Sign up today!



Structure, stability, and electronic property of carbon-doped gold clusters Au_nC^- ($n = 1-10$): A density functional theory study

Li-Li Yan,¹ Yi-Rong Liu,¹ Teng Huang,¹ Shuai Jiang,¹ Hui Wen,¹ Yan-Bo Gai,¹ Wei-Jun Zhang,^{1,2,a)} and Wei Huang^{1,2,a)}

¹Laboratory of Atmospheric Physico-Chemistry, Anhui Institute of Optics & Fine Mechanics, Chinese Academy of Sciences, Hefei, Anhui 230031, China

²School of Environmental Science & Optoelectronic Technology, University of Science and Technology of China, Hefei, Anhui 230026, China

(Received 11 October 2013; accepted 6 December 2013; published online 31 December 2013)

The equilibrium geometric structures, relative stabilities, and electronic properties of Au_nC^- and Au_{n+1}^- ($n = 1-10$) clusters are systematically investigated using density functional theory with hyper-generalized gradient approximation. The optimized geometries show that one Au atom capped on $\text{Au}_{n-1}\text{C}^-$ clusters is a dominant growth pattern for Au_nC^- clusters. In contrast to Au_{n+1}^- clusters, Au_nC^- clusters are most stable in a quasi-planar or three-dimensional structure because C doping induces the local non-planarity while the rest of the structure continues to grow in a planar mode, resulting in an overall non-2D configuration. The relative stability calculations show that the impurity C atom can significantly enhance the thermodynamic stability of pure gold clusters. Moreover, the effect of C atom on the Au_n^- host decreases with the increase of cluster size. The HOMO-LUMO gap curves show that the interaction of the C atom with Au_n^- clusters improves the chemical stability of pure gold clusters, except for Au_3^- and Au_4^- clusters. In addition, a natural population analysis shows that the charges in corresponding Au_nC^- clusters transfer from the Au_n^- host to the C atom. Meanwhile, a natural electronic configuration analysis also shows that the charges mainly transfer between the $2s$ and $2p$ orbitals within the C atom. © 2013 AIP Publishing LLC. [<http://dx.doi.org/10.1063/1.4852179>]

I. INTRODUCTION

In the past, bulk gold was an ignored element because of its chemical inertness. However, since Haruta first discovered the prominent catalytic reactivity of gold nano-clusters supported on oxide substrates,¹ considerable attention has been devoted to studying gold clusters for clarifying their catalytic mechanisms and controlling their catalytic activities.²⁻¹⁰ To date, the structures of small-to-medium sized pure gold clusters, Au_n^- , have been determined through a variety of joint experimental and theoretical studies.¹¹⁻²⁷ We have previously determined that the small-sized gold clusters, Au_n^- ($n = 4-12$), exhibit two-dimensional (2D) planar structure,¹¹⁻¹³ noting that the 2D to 3D structural transition occurs at $n = 12$, which has been proven by using argon tagging.¹⁴ The Au_n^- ($n = 16-18$) clusters exhibit a hollow cage shape^{15,16} and the Au_{20}^- cluster possesses a tetrahedral structure (the smallest gold pyramid).¹⁷ For medium-sized gold clusters, Au_{24}^- possesses a tubular structure,^{18,19} and core-shell structure appears in the size range of $n = 25-35$ ^{18,20-22} and $55-64$.²³⁻²⁶ However, the Au_n^- ($n = 36-54$) clusters have not been verified due to a lack of experimental and computational evidence. The electronic property as well as the structural evolution of the above Au_n^- clusters are summarized by Wang *et al.*²⁷

To enhance the stability of gold clusters and tune their chemical reactivity more precisely, a considerable amount of experimental and theoretical work has been implemented on gold clusters doped with impurity atoms, most commonly transition metal impurities. For example, Guo *et al.* reported the double-doped Au_nPd_2 and Au_nPt_2 ($n = 1-4$) clusters.^{28,29} Different from the single-doped analogue, the results show that the gold-impurity interaction is strong enough to change the known growth pattern of pure gold clusters, implying that the larger the clusters, the smaller the deformation caused by the two dopants. Compared with the Au_nM_2 ($M = \text{Pd}, \text{Pt}; n = 1-4$) clusters, Au_nNi_2 clusters show an inverse odd-even alternation phenomenon in magnetic property.³⁰ A density functional theory (DFT) study of Au_nM_2 ($M = \text{Si}, \text{P}; n = 1-8$) clusters³¹ indicates that the most stable isomers for Au_nSi_2 and Au_nP_2 ($n = 1-8$) clusters prefer a 3D structure when n is equal to or greater than 2 and 3, respectively. For single doping, Wang and co-workers reported that isoelectronic replacement of Au by Cu or Ag changes the onset of the 2D to 3D structural transition to a smaller size.³² Yuan *et al.* studied the Au_nM ($M = \text{Ni}, \text{Pd}, \text{Pt}$) clusters³³ and found that Ni cannot change the geometry of the host clusters, while for Pd- and Pt-doped Au clusters, the ground state structures change significantly. Dong *et al.* studied the Au_nM ($M = \text{Sc}, \text{V}, \text{and Mn}$) clusters³⁴⁻³⁶ and concluded that the ground state structures prefer a planar configuration with M occupying the higher coordination site. Li *et al.* reported that the lowest-energy structures of Au_nZn^- ($n = 2-10$) clusters³⁷ favor 2D configuration, as in the Au_n^- clusters.

^{a)} Authors to whom correspondence should be addressed. Electronic addresses: huangwei6@ustc.edu.cn and wjzhang@aiofm.ac.cn

Although a large number of studies have been focused on the transition metal-doped gold clusters, there have been relatively few studies on gold clusters with non-transition elements as dopants. Majumder and Kandalam³⁸ have proven that when gold clusters are doped with impurity elements possessing p electrons, the whole structure would prefer a three-dimensional (3D) configuration because of the sp^3 hybridization, which can be verified by gold clusters doped with various elements, such as Al, Si, P, and S.^{38–42} There are many studies on the gold clusters containing Si, Ge, and Sn elements. Though these dopants are from the same main group, there are two differences in the growth mode of Si-doped Au clusters from Ge- and Sn-doped clusters. On one hand, $Au_4Si^{-1/0}$ clusters exhibit T_d symmetry,⁴³ which are similar to $SiH_4^{-1/0}$,⁴⁴ viz., the Au/H analogue, which was later confirmed in other Si-doped gold clusters, such as $Au_2Si_4^{-1/0}$, $Au_2Si_2^{-1/0}$, and $Au_3Si_3^{-1/0/+1}$.^{45,46} However, Au_4Ge^- and Au_4Sn^- clusters have C_{4v} symmetry⁴⁷ rather than the T_d configuration; thus, the Au/H analogue does not exist in Au_4Ge^- and Au_4Sn^- clusters. On the other hand, the dopant atom in corresponding $Au_{16}X^-$ ($X = Si, Ge, \text{ and } Sn$) clusters is found to be exohedral ($X = Ge \text{ and } Sn$) or becomes a part of the gold cage ($X = Si$).^{48,49} In other words, the local structure around the dopant atom in the global minimum of $Au_{16}X^-$ ($X = Si, Ge, \text{ and } Sn$) clusters resembles the corresponding Au_4X clusters, which have a T_d geometry (Au_4Si) or a C_{4v} structure (Au_4Ge and Au_4Sn).⁴⁷ Moreover, the structure of $Au_{16}Si^-$ cluster has a dangling Au-Si unit, which reflects the competition between the tendency to form a Au_4Si local unit and the tendency to grow without destroying the integrity of the pure gold clusters. However, a DFT study shows that the lowest-energy structures of $Au_{16}C^{-1/0}$ clusters⁵⁰ are similar to those of $Au_{16}Ge^-$ and $Au_{16}Sn^-$ clusters in that they do not possess the local Au_4C unit with T_d geometry.⁴⁷ In addition, two DFT studies show that both $Au_4C^{-1/0}$ and $CH_4^{-1/0}$ clusters^{47,51} have T_d configuration, but whether there exists a Au/H analogy between them is still questionable. In short, in addition to theoretical calculation, experimental evidence is needed to further identify the global minimum of $Au_{16}C^{-1/0}$ and $Au_4C^{-1/0}$ clusters.

Though there are some studies^{47,50,52–58} on clusters that contain Au and C elements, as far as we know, there are relatively few systematic studies on the geometric structure, stability, and electronic property of C-doped Au clusters, which brings about an important question: are their structures and properties different from the pure gold or Si/Ge/Sn-doped Au clusters? In light of this question, this paper reports a systematic study of the geometries, stabilities, and electronic properties of Au_nC^- clusters by means of a density functional method. The goal of this work is to provide effective guidelines for future experimental studies and contribute to further understanding the structures and electronic properties of C-doped Au clusters, which may be useful in creating a new type of C-Au nanostructure for nanocatalysis.

II. COMPUTATIONAL METHODS

The calculations were carried out in three steps. In the first step, we used the basin-hopping (BH) algorithm^{59–61} cou-

pled with DFT in the DMol3 software package⁶² to search the potential energy surfaces of Au_nC^- ($n = 1–10$) clusters at the BLYP/DNP (DNP is the abbreviation of double-numerical polarized basis set) level of theory. After the BH global search program, we chose a few tens of low-energy isomers for each species from a few hundreds searched structures. Then, we ran the second step (optimization), implemented in the NWChem 6.0 software package,⁶³ in which the generalized gradient approximation (GGA) in the Perdew-Burke-Ernzerhof (PBE) functional form was chosen. All of the low-lying structures were optimized at the PBE/aug-cc-pVDZ(AVDZ) level of theory. Additionally, the scalar relativistic effective core potential and the CRENL basis set are for the Au atom in the present work, except for the (U)CCSD(T)-F12 calculation in Tables I and II. Next, we selected a few of low-lying isomers for re-optimization at the PBE0/aug-cc-pVTZ(AVTZ) level of theory. To verify the stability of each isomer, we calculated the harmonic vibrational frequency using the GAUSSIAN 09 program,⁶⁴ which is at the same theoretical level as the second-run optimization. If an imaginary vibrational mode appears, a relaxation along the coordinates of the imaginary vibrational mode will be performed until the true minimum is actually obtained.

It is well known that relativistic effects play an important role in the growth pattern of gold clusters.^{65–71} The preference for planar structure of gold clusters has been attributed to strong relativistic effects, which enhance the s - d hybridization by stabilizing the $6s$ orbital and destabilizing the $5d$ orbital of the Au atom. Therefore, to obtain accurate information regarding the Au_nC^- ($n = 1–10$) clusters, the spin-orbit (SO) effects^{72–74} were included in the single-point energy calculation, which was based on the re-optimized structures at the SO-PBE0/AVTZ level of theory in the NWChem 6.0 software package. Additionally, inclusion of the SO effects can make the computed photoelectron spectroscopy (PES) more in line with the experimental data.^{32,75–80} The first vertical detachment energy (VDE) was calculated as the energy difference

TABLE I. Relative (U)CCSD(T)-F12/6-31+G* energies^a (in kcal/mol) based on the optimized geometries of Au_nC^- ($n = 2–5$) clusters at the PBE0/AVTZ and B3LYP/6-311+G* levels of theory.

Cluster size	Isomers	PBE0/AVTZ	B3LYP/6-311+G*
n = 2	Isomer 1	0.000	0.647
	Isomer 2	0.000	0.419
n = 3	Isomer 1	0.000	1.366
	Isomer 2	0.000	0.799
n = 4	Isomer 1	0.000	1.020
	Isomer 2	0.000	1.537
	Isomer 3	0.000	0.438
	Isomer 4	0.000	6.456
n = 5	Isomer 1	0.000	1.529
	Isomer 2	0.000	2.360
	Isomer 3	0.000	1.108
	Isomer 4	0.000	2.109

^aThe (U)CCSD(T)-F12 calculations are performed in MOLPRO 2010.1. CCSD(T)-F12 is for close-shell construction and UCCSD(T)-F12 is for open shell. In addition, the aug-cc-pVTZ-pp basis set is for Au and 6-31+G* is for the C atom. The lowest energy for each of the corresponding isomers is set to 0.000 kcal/mol.

TABLE II. The computed relative energies^a (in kcal/mol) of the top several low-lying isomers at the SO-PBE0/AVTZ, SO-B3LYP/6-311+G*, and (U)CCSD(T)-F12/6-31+G* levels of theory.^b The computed relative energies of these three levels of theory are all based on the optimized geometries of clusters at the PBE0/AVTZ level of theory.

Au ₂ C ⁻	Isomer 1	Isomer 2	Isomer 3	Isomer 4
Δ E [SO-PBE0/AVTZ]	0.000	14.395
Δ E [SO-B3LYP/6-311+G*]	0.000	0.000
Δ E [UCCSD(T)-F12/6-31+G*]	0.000	15.749
Au ₃ C ⁻	Isomer 1	Isomer 2	Isomer 3	Isomer 4
Δ E [SO-PBE0/AVTZ]	0.000	6.976
Δ E [SO-B3LYP/6-311+G*]	0.000	5.072
Δ E [CCSD(T)-F12/6-31+G*]	0.000	13.227
Au ₄ C ⁻	Isomer 1	Isomer 2	Isomer 3	Isomer 4
Δ E [SO-PBE0/AVTZ]	0.000	13.994	13.994	18.046
Δ E [SO-B3LYP/6-311+G*]	8.699	19.235	0.000	21.220
Δ E [UCCSD(T)-F12/6-31+G*]	0.000	11.637	1.649	18.615
Au ₅ C ⁻	Isomer 1	Isomer 2	Isomer 3	Isomer 4
Δ E [SO-PBE0/AVTZ]	0.000	14.874	27.242	27.242
Δ E [SO-B3LYP/6-311+G*]	4.922	22.597	23.934	0.000
Δ E [CCSD(T)-F12/6-31+G*]	0.000	18.427	32.126	20.208

^aThe lowest energy for each of the corresponding isomers is set to 0.000 kcal/mol.

^bThe SO-PBE0/AVTZ and SO-B3LYP/6-311+G* calculations are performed using the NWChem 6.0 software package. The CRENL ECP basis set is for the Au atom in both levels of theory. The calculation situation for (U) CCSD(T)-F12 is the same as that in Table I.

between the anionic and neutral species of each isomer based on the corresponding anion geometry. The binding energies of the deeper occupied orbitals of the anion were then added to the first VDE to give VDEs for the excited states. The simulated PES was obtained by fitting the computed VDEs with Gaussian functions of 0.04 eV widths. The highest occupied-lowest unoccupied molecular orbital (HOMO-LUMO) gaps of the most stable isomers of Au_nC⁻ (n = 1–10) clusters were also obtained in NWChem 6.0. We also gained reliable charge-transfer information by natural population analysis (NPA) from natural bond orbital (NBO) analysis^{81,82} in GAUSSIAN 09.

To test the reliability of the combination of PBE0 and AVTZ for the optimization and single-point energy calculations, we performed a simple comparison with the B3LYP (Becke's three-parameter hybrid exchange functional with the Lee-Yang-Parr nonlocal correlation functional)/6-311+G* group. These two types of functionals are popular methods and have been proven to be effective tools for the investigation of included-gold clusters. First, we calculated the (U)CCSD(T)-F12/6-31+G* (the aug-cc-pVTZ-pp basis set is for the Au atom) energies^{83–86} (see Table I) based on the optimized geometries of clusters at both PBE0/AVTZ and B3LYP/6-311+G* levels of theory in MOLPRO 2010.1.⁸⁷ The calculation results of several isomers in Au_nC⁻ (n = 2–5) clusters showed that the energies of geometries optimized at the PBE0/AVTZ level of theory are lower than those of geometries based on the B3LYP/6-311+G* level, indicating that the structures after optimization of the PBE0/AVTZ union obtained more sufficient optimization and may be located at a lower site on the potential energy surface. Thus, we selected the PBE0/AVTZ union for optimization. Second, we com-

puted the corresponding energies at the SO-PBE0/AVTZ, SO-B3LYP/6-311+G*, and (U)CCSD(T)-F12/6-31+G* levels of theory based on the optimized geometries at the PBE0/AVTZ level of theory. The results are shown in Table II. Through the comprehensive consideration of the confirmation of the lowest-energy structure, the energy order, and the energy difference from the (U)CCSD(T)-F12 energy, we concluded that the performance of SO-PBE0/AVTZ union was better than that of SO-B3LYP/6-311+G* aside from several defects. Thus, we select the PBE0/AVTZ group for optimization and single-point energy calculations in the present work. Although it is difficult to confirm that we have achieved the lowest-energy structures of Au_nC⁻ (n = 1–10) clusters because of the lack of experimental data, it is worth mentioning that we have performed an extensive search to the best of our ability.

III. RESULTS AND DISCUSSIONS

A. Structures and VDEs

To study the effect of impurity atom on gold clusters, we first performed some optimization and energy calculations on pure gold clusters, Au_{n+1}⁻ (n = 1–10), by using the same method, basis set, and software as in Au_nC⁻ clusters. Although many possible initial structures were taken into account, only the most stable isomers for each size were selected and shown in Figs. 1 and 2. A few low-energy isomers are listed in Table S1.⁸⁸ It is interesting to note that the geometric structures are in good agreement with the previous results.^{11,12,27,78,79,89,90} It is also necessary to illustrate that the W-like and triangle-like structures (see Table S1)⁸⁸ are the lowest in energy for the Au₅⁻ cluster. To affirm the global minimum, we calibrated the single-point energy at the CCSD(T)-F12/6-31+G* level of theory in MOLPRO 2010.1. The results reveal that the W-like structure is more stable than the triangle structure by 0.005 eV. Moreover, the calculated VDE value of W-like structure is 2.89 eV, which is in good agreement with the experimental values (2.98 eV⁹¹ and 3.09 eV¹²), while the corresponding value of triangle structure is 3.62 eV, far larger than the experimental value. Thus, the W-like structure is actually the global minimum for the Au₅⁻ cluster. For the Au₆⁻ cluster, the recognized lowest-energy structure in previously published literature is the triangle configuration,^{11,12,89,90} which is the second lowest-energy structure in the present work (see Table S1),⁸⁸ unfortunately. Moreover, the triangle structure is 0.225 eV higher in energy than the cart-like ground-state structure. To confirm the global minimum in theory, we performed higher level single-point energy calculation for the first three lowest-energy structures at the MP2/AVTZ level of theory in NWChem 6.0. The MP2 calculation results show that the triangle structure is more stable than the cart-like and hat-like structures by 0.371 and 0.214 eV, respectively. Furthermore, the computed VDE value (1.83 eV) of the triangle structure is in reasonable agreement with the experimental values (2.00 eV⁹¹ and 2.13 eV¹²), while the corresponding VDE values of the other two isomers are 3.41 eV (for the cart-like structure) and 2.40 eV (for the hat-like structure). Thus, we adopt the triangle structure in the present work. Additionally, the averaged atomic



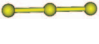
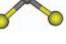
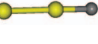



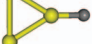


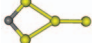









		-	-	-	-
Au ₂ ⁻ D _{∞h}	1a, C _{∞v}	-	-	-	-
			-	-	-
Au ₃ ⁻ D _{3h}	2a, C _{2v} 0.000	2b, C _s 0.624	-	-	-
				-	-
Au ₄ ⁻ C _{2v}	3a, C _{3v} 0.000	3b, C ₁ 0.302	3c, C _s 0.302	-	-
					
Au ₅ ⁻ C _{2v}	4a, C _s 0.000	4b, C _s 0.607	4c, C ₁ 0.607	4d, C _s 0.783	4e, C _s 0.783
					
Au ₆ ⁻ C _{3h}	5a, C _{3v} 0.000	5b, C ₁ 0.645	5c, C _s 0.645	5d, C _s 1.181	5e, C _s 1.181

FIG. 1. Lowest-energy structures of Au_nC⁻ and Au_{n+1}⁻ (n = 1–5) clusters and a few of the low-lying isomers for doped clusters at the SO-PBE0/AVTZ//PBE0/AVTZ level of theory. The first number represents the cluster size and the data after the comma represent the geometry symmetries and the relative energies (in eV) with respect to the ground state isomers for Au_nC⁻ (n = 1–5) clusters.





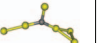



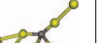
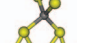

























						
Au ₇ ⁻ C _{2v}	6a, C _s 0.000	6b, C _s 0.415	6c, C _{2v} 0.415	6d, C ₁ 0.489	6e, C ₁ 0.489	6f, C ₁ 0.498
						
Au ₈ ⁻ C _{4h}	7a, C ₁ 0.000	7b, C ₁ 0.000	7c, C ₁ 0.192	7d, C _s 0.356	7e, C ₁ 0.359	7f, C ₁ 0.525
						
Au ₉ ⁻ C _{2v}	8a, C ₁ 0.000	8b, C ₁ 0.154	8c, C ₁ 0.406	8d, C ₁ 0.538	8e, C ₁ 0.648	8f, C ₁ 0.650
						
Au ₁₀ ⁻ C ₁	9a, C ₁ 0.000	9b, C ₁ 0.159	9c, C _s 0.164	9d, C ₁ 0.299	9e, C ₁ 0.312	9f, C ₁ 0.420
						
Au ₁₁ ⁻ C ₁	10a, C ₁ 0.000	10b, C ₁ 0.005	10c, C _s 0.005	10d, C ₁ 0.020	10e, C ₁ 0.143	10f, C ₁ 0.149

FIG. 2. Lowest-energy structures of Au_nC⁻ and Au_{n+1}⁻ (n = 6–10) clusters and a few of the low-lying isomers for doped clusters at the SO-PBE0/AVTZ//PBE0/AVTZ level of theory. The first number represents the cluster size and the data after the comma represent geometry symmetries and the relative energies (in eV) with respect to the ground state isomers for Au_nC⁻ (n = 6–10) clusters.

TABLE III. Point group symmetry and the computed first VDEs of the lowest-energy Au_nC^- and Au_{n+1}^- ($n = 1-10$) clusters, along with the experimental VDE values of Au_{n+1}^- ($n = 1-10$) clusters in Refs. 12, 91, and 95. All of energies are in eV.

Cluster size	Au_nC^-		Au_{n+1}^-				
	Symmetry	VDE (Calc.)	Symmetry	VDE (Calc.)	VDE (Expt. ^a)	VDE (Expt. ^b)	VDE (Expt. ^c)
$n = 1$	$\text{C}_{\infty\text{v}}$	1.23	$\text{D}_{\infty\text{h}}$	1.89	2.01(3)	1.90	2.01 ± 0.01
$n = 2$	$\text{C}_{2\text{v}}$	2.04	$\text{D}_{\infty\text{h}}$	3.49	3.88(2)	3.77	...
$n = 3$	$\text{C}_{3\text{v}}$	2.81	$\text{C}_{2\text{v}}$	2.64	2.75(3)	2.63	2.79 ± 0.05
$n = 4$	C_s	2.00	$\text{C}_{2\text{v}}$	2.89	3.09(3)	2.98	3.12 ± 0.05
$n = 5$	$\text{C}_{3\text{v}}$	3.60	$\text{C}_{3\text{h}}$	1.83	2.13(2)	2.00	...
$n = 6$	C_s	2.80	$\text{C}_{2\text{v}}$	3.26	3.46(2)	3.38	...
$n = 7$	C_1	3.29	$\text{C}_{4\text{h}}$	2.69	2.79(2)	2.79	...
$n = 8$	C_1	2.98	$\text{C}_{2\text{v}}$	3.69	3.83(2)	3.78	...
$n = 9$	C_1	3.59	C_1	3.80	3.91(2)	2.98	...
$n = 10$	C_1	3.51	C_1	3.60	3.80(2)	3.71	...

^aReference 12. The numbers in parentheses represent the experimental uncertainties in the last digits.

^bReference 91.

^cReference 95.

binding energies, attachment energies, second-order difference of energies, the first VDEs, and the HOMO-LUMO gaps of pure gold clusters are also calculated and compared with the available experimental values.

1. Structures

Figure 1 shows the lowest-energy structures of Au_nC^- and Au_{n+1}^- ($n = 1-5$) clusters in addition to a few of low-lying isomers for doped gold clusters at the SOPBE0/AVTZ//PBE0/AVTZ level of theory. The corresponding structures of Au_nC^- and Au_{n+1}^- clusters for $n = 6-10$ are shown in Fig. 2. According to the total energy from lowest to highest, the low-lying isomers are designated by na, nb, nc, nd, ne, and nf, where n is the number of Au atoms in the clusters. Meanwhile, the symmetries and relative energies with respect to each of the corresponding ground-state isomers are also presented in Figs. 1 and 2. Moreover, the VDE values are listed in Table III, HOMO-LUMO gaps are shown in Table IV, and the corresponding computed PES are shown in Figs. S2-S10.⁸⁸

Regarding the ground-state geometries of the Au_nC^- ($n = 1-10$) clusters, our calculation results show that the equilibrium bond length of Au-C in the Au_1C^- cluster is 1.818 Å, which is smaller than the calculated value of Au-Au (2.660 Å) in the Au_2^- cluster. This is because the radius of a C atom is less than that of a Au atom. The lowest-energy isomer (2a) of the Au_2C^- cluster is an isosceles triangle structure with $\text{C}_{2\text{v}}$ symmetry and an apex angle of 101.01° , which resembles the lowest-energy structures of Au_2Si^- ⁴³ and Au_2Sn clusters.⁹² A linear chain structure (2b) with the C atom located at the edge of the Au-Au bond is 0.642 eV higher in energy than Isomer 2a. The chain structure can be obtained by adding one Au atom connecting to the Au atom of Isomer 1a, one C atom on the edge of the Au_2^- cluster, or by replacing a side Au atom in the Au_3^- cluster. In addition, the triangle structure can be taken as Au_1C^- with another Au atom binding with the C atom.

For the Au_3C^- cluster, a 3D structure (3a) is found to be the global minimum with $\text{C}_{3\text{v}}$ symmetry and different Au-C bond lengths (1.951, 1.951, and 1.960 Å), which is

TABLE IV. HOMO/LUMO energies and the gaps between them for the lowest-energy Au_nC^- and Au_{n+1}^- ($n = 1-10$) clusters. All of energies are in eV.

Cluster size	Au_nC^-			Au_n^-		
	HOMO	LUMO	HOMO-LUMO gap	HOMO	LUMO	HOMO-LUMO gap
$n = 1$	0.45749	2.76133	2.30
$n = 2$	-0.46645	2.17268	2.64	-0.20936	1.81008	2.02
$n = 3$	-1.42370	1.72186	3.15	-1.91898	1.50476	3.42
$n = 4$	-0.71031	0.86735	1.58	-1.19581	0.67913	1.87
$n = 5$	-2.25984	0.49962	2.76	-1.51188	0.81033	2.32
$n = 6$	-1.61541	0.37485	1.99	-1.11419	0.27038	1.38
$n = 7$	-2.09568	0.33701	2.43	-2.00871	0.20984	2.22
$n = 8$	-1.91503	-0.25391	1.66	-1.55365	-0.34941	1.20
$n = 9$	-2.47233	-0.15066	2.32	-2.48586	-0.40053	2.09
$n = 10$	-2.48132	-0.51920	1.96	-2.68092	-1.46654	1.21
$n = 11$	-2.51125	-0.53154	1.98

similar to the lowest-energy structures of Au_3Si^- and Ag_3C^- clusters.^{43,93} The structure of Isomer 3a can be obtained from Isomer 2a after another Au atom connecting to the C atom. Meanwhile, the calculation shows that the second lowest-energy structures are an ax-like structure (3b) and a Y-shaped structure (3c), which are entirely degenerate (0.302 eV for both of them). The former can be taken as the Isomer 2a or 2b with a Au atom added to the corresponding site of these isomers, and the latter can be considered to be the Au_4^- cluster with a C atom replacing the top Au atom.

In the case of the Au_4C^- cluster, a distorted tetrahedron configuration (4a) is proven to be the global minimum with C_s symmetry, which can be described as Isomer 3a after another Au atom connecting to the C atom. Additionally, if another Au atom connects to the Au atom in Isomer 3a, a new isomer (4e) with C_s symmetry will emerge, which is 0.783 eV higher in energy than Isomer 4a. However, a DFT study shows that the Au_4C^- cluster has T_d symmetry⁴⁷ rather than C_s symmetry, thus the true global minimum for the Au_4C^- cluster is still unknown, further emphasizing the necessity of the relevant experiments.

Among the stable isomers of the Au_5C^- cluster, an isomer (5a) with C_{3v} symmetry is proven to be the ground state, which is derived from Isomer 4a with one Au atom top-capped and has the same structure as the Au_5Si^- cluster.⁹⁴ Moreover, four other isomers (5b, 5c, 5d, and 5e) are taken into account with different symmetries and relative energies from Isomer 5a (C_1 , 0.645 Å; C_s , 0.645 Å; C_s , 1.181 Å; and C_s , 1.181 Å; respectively).

When one central Au atom is replaced by a C atom in the second lowest-energy structure of the Au_7^- cluster (see Table S1),⁸⁸ another isomer (6a) will be generated with C_s symmetry. As a result of the incorporation of the C atom, six Au atoms in Isomer 6a are no longer coplanar. Additionally, it can be observed from Fig. 2 that the energy of Isomer 6b is higher than that of Isomer 6a by 0.415 eV. Furthermore, Isomers 6b and 6f can also be obtained by adding one Au atom to Isomers 5b and 5c, respectively.

In our search for the global minimum of the Au_7C^- cluster, we find two 3D structures (7a, 7b) to be the lowest in energy and entirely degenerate. Both of them are lowly symmetrical (C_1), and the former can be taken as Isomer 6d with one added-Au atom binding with the C atom, and the latter is the analogous structure of Isomer 6a by the same manner. Moreover, Isomer 6a has another derivative, Isomer 7c, that is top-capped with a Au atom. To obtain the global minimum in theory, we conducted higher level MP2/AVTZ single-point energy calculation in NWChem 6.0, which showed that Isomer 7b is more stable than Isomer 7a by 0.545 eV; thus, we chose Isomer 7b as the global minimum in the present work.

For the Au_8C^- cluster, a deformed planar structure (8a) is found to be the global minimum with C_1 symmetry, which can be derived from the Au_8^- cluster by a dangling C-Au unit replacing one of the top Au atoms. Moreover, if a C atom displaces a bottom Au atom in the Au_9^- cluster and then the overall structure undergoes partial structural relaxation, a new structure (8c) will form.

According to our calculations, the lowest-energy structure of the Au_9C^- cluster possesses the same symmetry (C_1) as Isomer 8a, and the overall structure is derived from 8a by the addition of a Au atom binding with the C atom. Additionally, Isomer 8c has two derivatives (9b and 9f) in which another Au atom binds with the Au or C atom, respectively.

As for the Au_{10}C^- cluster, the global minimum is still non-planar, which can be visualized as Isomer 9b with an added-Au atom binding with the C atom. At the same time, Isomer 9b has another derivative (10e) after being capped by a Au atom. Furthermore, if a Au atom binds with the dangling Au atom in Isomer 9a, another structure (10f) will emerge.

On the basis of the above discussion regarding Au_nC^- ($n = 1-10$) clusters, it is remarkable that the lowest-energy structures favor 3D configuration for $n = 3, 4, 5, 7$, and 9 ; quasi-2D configuration for $n = 6, 8$, and 10 ; and, as expected, 1D for Au_1C^- and 2D for Au_2C^- cluster. To gain insight on the structural evolution of these Au_nC^- clusters, the extent of dimensionality change has been measured by using the average dihedral angle of the C atom with respect to the connected Au atoms in Mercury 3.1. These values are summarized in Table S2.⁸⁸ In addition, the coordination numbers of the C atoms and the average Au-C bond lengths are also shown in this table. As seen from Table S2,⁸⁸ we can draw a conclusion that the degree of dimensionality change only depends on the Au-C dangling unit in Au_nC^- ($n = 6-10$) clusters. Also, the extent of dimensionality change of clusters with only one Au-C dangling unit will be smaller than that of clusters with two Au-C dangling units (see the supporting information for detailed analysis).

Combining Figs. 1 and 2, and Table S2,⁸⁸ we can conclude that the lowest-energy structures of Au_nC^- ($n = 1-10$) clusters are not purely planar configurations anymore, except for the $\text{Au}_{1,2}\text{C}^-$ clusters. Furthermore, the C doping induces local non-planarity, while the rest of the structure continues to grow in a planar mode, resulting in an overall quasi-2D or 3D structure. Therefore, the doped C atom dramatically changes the ground-state geometries of Au_n^- ($n = 1-10$) clusters. Moreover, one Au atom capped on a $\text{Au}_{n-1}\text{C}^-$ structure is the dominant growth pattern for Au_nC^- clusters.

2. VDEs

The computed first VDE values of the lowest-energy Au_nC^- and Au_{n+1}^- ($n = 1-10$) clusters, along with the experimental VDE values of the Au_{n+1}^- ($n = 1-10$) clusters in previous literatures,^{11,12,91,95} are listed in Table III. The corresponding curves for the cluster size, n , are presented in Fig. 3, where only the experimental data from Refs. 12 and 91 are shown because of the considerably detailed experimental and theoretical data. From Fig. 3, we can see that the computed VDE values of Au_{n+1}^- ($n = 1-10$) clusters are generally lower than the experimental values, and generally present the odd-even alternation phenomenon with the exception of the Au_{10}^- cluster.

As for the Au_{10}^- cluster, there are two very weak features at 2.98 and 3.5 eV in the photoelectron spectrum,^{12,91} with the first weak peak being attributed to the first VDE value of the

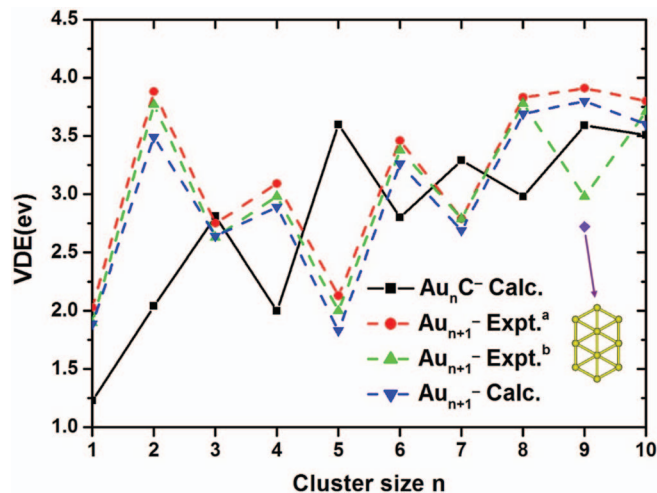


FIG. 3. Size dependence of the computed first VDEs of the lowest-energy structures for Au_nC^- and Au_{n+1}^- ($n = 1-10$) clusters, along with the experimental VDE values of Au_{n+1}^- ($n = 1-10$) clusters in Refs. 12 and 91, which are in line with those in Table III. All energies are in eV. In addition, the violet square frame stands for the theoretical value for one of the Au_{10}^- clusters, and the inset shows the corresponding structure.

cluster in Refs. 11 and 91. However, our calculations show that the triangular structure is the global minimum with the VDE value of 3.80 eV, which is smaller than the first strong PES peak by 0.11 eV. This difference in values is within the range of 0.1–0.3 eV when the SO effects are included in the single-point energy calculation, as shown in Ref. 78. Moreover, the difference of experimental spectra between the Au_9^- and Au_{10}^- clusters is very small, implying that the structural change between them is equally small. Thus, there is little doubt that the triangular structure is the global minimum. In the present work, a planar structure with C_2 symmetry (the third lowest-energy structure of the Au_{10}^- cluster in Table S1⁸⁸) has the VDE value of 2.72 eV and is identified as the minor isomer because of the excellent agreement with the first weak peak. The corresponding structure is also shown in the inset of Fig. 3, and the violet square frame stands for the theoretical VDE value. From Fig. 3, we can see that the corresponding experimental and theoretical values for these two isomers are in agreement, which also reflects the structural sensibility of VDE.

For Au_nC^- ($n = 1-10$) clusters, the VDE values also follow the odd-even alternation phenomenon, with the exception of the Au_1C^- cluster. The Au_1C^- cluster has the smallest VDE value of 1.23 eV, which suggests that only 1.23 eV is required to remove an extra electron from the Au_1C^- cluster by means of photoelectron spectroscopy. At the same time, Au_5C^- has the largest VDE value of 3.60 eV. By comparison of the VDE values of Au_nC^- and Au_{n+1}^- ($n = 1-10$) clusters, we can see that there is no obvious relationship between them. In addition, the VDE values at the same cluster size are anti-correlative on the whole because of the typical odd-even electronic effect: Au_nC^- clusters have three valence electrons more than the corresponding Au_{n+1}^- clusters. Unfortunately, there has been no experimental VDE data for Au_nC^- clusters until now. Thus, more efforts need to be fully invested in the theoretical and experimental studies on them.

B. Relative stabilities

To predict the relative stabilities of Au_nC^- and Au_{n+1}^- ($n = 1-10$) clusters, the average atomic binding energies, $E_b(n)$; Au attachment energies, $\Delta_{\text{Au}}E(n)$; C attachment energies, $\Delta_{\text{C}}E(n)$; and the second-order difference of energies, $\Delta_2E(n)$, for the lowest-energy structures of these two kinds of clusters are calculated. For Au_nC^- clusters, $E_b(n)$, $\Delta_{\text{Au}}E(n)$, $\Delta_{\text{C}}E(n)$, and $\Delta_2E(n)$ are defined as follows:

$$E_b(n) = \frac{E(\text{C}^-) + nE(\text{Au}) - E(\text{Au}_n\text{C}^-)}{n+1}, \quad (1)$$

$$\Delta_{\text{Au}}E(n) = E(\text{Au}_{n-1}\text{C}^-) + E(\text{Au}) - E(\text{Au}_n\text{C}^-), \quad (2)$$

$$\Delta_{\text{C}}E(n) = E(\text{Au}_n^-) + E(\text{C}) - E(\text{Au}_n\text{C}^-), \quad (3)$$

$$\Delta_2E(n) = E(\text{Au}_n\text{C}^-) + E(\text{Au}_{n+1}\text{C}^-) - 2E(\text{Au}_n\text{C}^-), \quad (4)$$

where $E(\text{Au})$, $E(\text{C})$, $E(\text{C}^-)$, $E(\text{Au}_n^-)$, $E(\text{Au}_{n-1}\text{C}^-)$, $E(\text{Au}_n\text{C}^-)$, and $E(\text{Au}_{n+1}\text{C}^-)$ denote the total energy of Au, C, C^- , Au_n^- , $\text{Au}_{n-1}\text{C}^-$, Au_nC^- , and $\text{Au}_{n+1}\text{C}^-$ clusters, respectively. For Au_n^- clusters, $E_b(n)$, $\Delta_{\text{Au}}E(n)$, and $\Delta_2E(n)$ are defined as follows:

$$E_b(n) = \frac{E(\text{Au}^-) + (n-1)E(\text{Au}) - E(\text{Au}_n^-)}{n}, \quad (5)$$

$$\Delta_{\text{Au}}E(n) = E(\text{Au}) + E(\text{Au}_{n-1}^-) - E(\text{Au}_n^-), \quad (6)$$

$$\Delta_2E(n) = E(\text{Au}_{n-1}^-) + E(\text{Au}_{n+1}^-) - 2E(\text{Au}_n^-), \quad (7)$$

where $E(\text{Au})$, $E(\text{Au}^-)$, $E(\text{Au}_n^-)$, $E(\text{Au}_{n-1}^-)$, and $E(\text{Au}_{n+1}^-)$ denote the total energy of Au, Au^- , Au_n^- , Au_{n-1}^- , and Au_{n+1}^- clusters, respectively.

The $E_b(n)$, $\Delta_{\text{Au}}E(n)$, $\Delta_{\text{C}}E(n)$, and $\Delta_2E(n)$ values of the lowest-energy structures for Au_nC^- and Au_{n+1}^- ($n = 1-10$) clusters measured against the corresponding cluster size, n , are plotted in Fig. 4. In general, the average atomic binding energies, $E_b(n)$, of Au_nC^- clusters are higher than those of the corresponding Au_{n+1}^- clusters, indicating that the substitution of Au by C atom in the Au_{n+1}^- clusters leads to the improvement of overall relative stability. The enhanced-stability effect of the C atom is most prominent for Au_1C^- and Au_2^- clusters, whose binding energies are 1.01 and 2.27 eV, respectively. The variation trend of $E_b(n)$ for Au_nC^- clusters is to increase until $n = 3$ and then follows a plateau down to $n = 10$ with very small peaks or hollows for specific clusters, reflecting their relative stabilities. The clusters with an odd number of Au atom are more stable than even-numbered clusters, excluding the Au_1C^- cluster. The odd-even alternation phenomenon can be explained by the electron pairing effect. As for Au_{n+1}^- ($n = 1-10$) clusters, though $E_b(n)$ values do not present an odd-even nature, the overall change trend is rising. Regardless of whether the average atomic binding energies of Au_nC^- and Au_{n+1}^- ($n = 1-10$) clusters increase, they exhibit a convergent tendency close to a limit, which reflects the fact that the larger the clusters, the smaller the effect of impurity on the host framework. Additionally, a large jump appears between the Au_1C^- and Au_2C^- clusters, the Au_2^- and Au_3^-

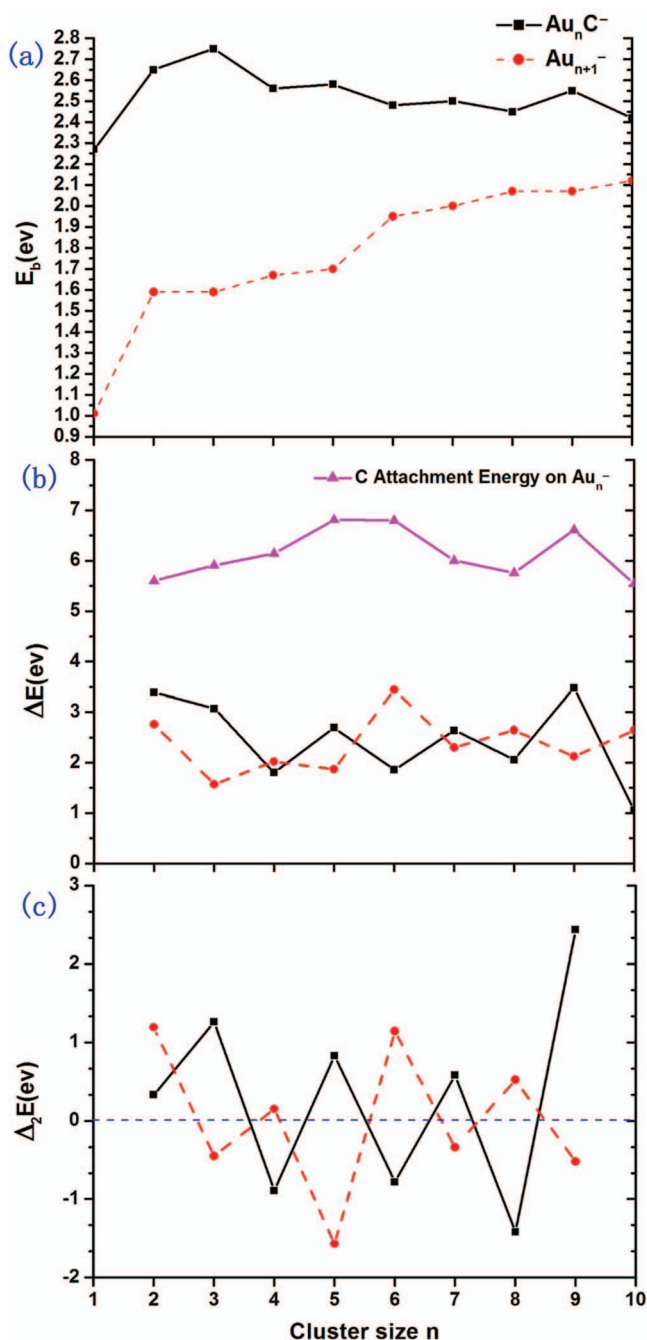


FIG. 4. Size dependence of the average atomic binding energies, $E_b(n)$ (a); Au attachment energies (C attachment energies, $\Delta_C E(n)$, of $Au_n C^-$ clusters marked with the filled triangles), $\Delta_{Au} E(n)$ (b); and the second-order difference of energies, $\Delta_2 E(n)$ (c), for the lowest-energy structures of $Au_n C^-$ and Au_{n+1}^- ($n = 1-10$) clusters.

clusters, respectively, indicating that the $Au_2 C^-$ and Au_3^- clusters exhibit a skipping increase of relative stability.

It is well known that the attachment energies, $\Delta_{Au} E(n)$ and $\Delta_C E(n)$, along with the second-order difference of energies, $\Delta_2 E(n)$, are sensitive indicators of the relative stability. The attachment energies of Au or C atoms on the specific size cluster stand for its ability towards spontaneous single-atom dissociation. The corresponding attachment energy curves as a function of the cluster size, n , are shown in Fig. 4(b). It is clear that the interaction of C atom with Au_n^-

clusters is energetically more favorable than the Au atom with Au_n^- or $Au_{n-1} C^-$ clusters. That is, the dissociation of C atom from $Au_n C^-$ clusters requires more energy than that of Au atom from $Au_n C^-$ or Au_{n+1}^- clusters because the attachment energies of C are larger than those of Au. Combined with Fig. 4(a), we can see that the impurity C atom can significantly enhance the stability of pure gold clusters, which is the purpose of the study on gold clusters doped with impurity atom. We have also compared the Au attachment energies of Au_{n+1}^- and $Au_n C^-$ clusters, and the results show that both of them obey the odd-even alternation phenomenon, which can be explained by the odd-even electron pairing effect. Additionally, because $Au_n C^-$ clusters have three valence electrons more than the corresponding Au_{n+1}^- clusters, it is very easy to understand that the variation trends are anti-correlative. To our surprise, the open-shell $Au_2 C^-$ cluster is unexpectedly more stable than the close-shell $Au_3 C^-$ cluster. The NBO analysis^{81,82} in GAUSSIAN 09 shows that the average Wiberg bond order⁹⁶⁻⁹⁹ of Au-C bond are 1.1276 a.u. and 1.0903 a.u. in the $Au_2 C^-$ and $Au_3 C^-$ clusters, respectively, implying that the extent of electron cloud overlap of Au and C atoms in $Au_2 C^-$ is larger than that in the $Au_3 C^-$ cluster, i.e., the interaction of Au and C atoms in $Au_2 C^-$ is stronger. Intuitively, the Au-C bond length of the $Au_2 C^-$ cluster (1.959 Å) is smaller than that of the $Au_3 C^-$ cluster (1.993 Å). Thus, there is no question of the higher attachment energy of Au atom in the $Au_2 C^-$ cluster in spite of the odd numbers of electrons. Furthermore, for $n = 2, 3, 5, 7$, and 9 , it is found that the dissociation of Au from $Au_n C^-$ clusters requires more energy than that from Au_{n+1}^- clusters; however, this trend is reversed for $n = 4, 6, 8$, and 10 . The reason for such a difference is the close-shell system for $Au_n C^-$ clusters at $n = 3, 5, 7$, and 9 , and the open-shell structures for Au_{n+1}^- clusters in the same size. Certainly, $n = 2$ is an exception because of its surprisingly high stability.

According to the total energy calculations, it is possible to confirm few stable clusters by plotting the second-order difference of energies as a function of cluster size, n . On the basis of the definition, as illustrated by Eqs. (4) and (7), one can determine that the clusters with positive $\Delta_2 E(n)$ values would be more stable than their vicinity clusters. The odd-even electron pairing effect in the relative stabilities of Au_{n+1}^- ($n = 2-9$) clusters can be reflected by the sharp oscillation of the $\Delta_2 E(n)$ values in Fig. 4(c). However, the appearance of the C atom changes the pattern for a series of clusters. The $Au_n C^-$ ($n = 2-9$) clusters with odd numbers of Au atoms are more stable than even-number clusters, except for the $Au_2 C^-$ cluster. The exceptional stability of the $Au_2 C^-$ cluster is in line with that in Fig. 4(b). In addition, the maximum $\Delta_2 E(n)$ value of $Au_n C^-$ ($n = 2-9$) clusters is found at $n = 9$.

In conclusion, the relative stabilities of $Au_n C^-$ and Au_{n+1}^- ($n = 1-10$) clusters have been verified based on various energy parameters, namely, average atomic binding energies, $E_b(n)$, atom attachment energies, $\Delta_{Au,C} E(n)$, and second order difference in energy, $\Delta_2 E(n)$, as shown in Fig. 4. The higher atomic binding energies of $Au_n C^-$ over Au_{n+1}^- ($n = 1-10$) clusters (see Fig. 4(a)), along with the higher C atom attachment energy over Au attachment energy (see Fig. 4(b)), reflect that the impurity C atom can greatly

enhance the relative stability of pure gold clusters. This is the purpose of the study on gold clusters doped with impurity atoms, including C atom. Moreover, the convergent tendency of average atomic binding energies for Au_nC^- and Au_{n+1}^- clusters (see Fig. 4(a)) suggests that the larger the clusters, the smaller the effect of impurity atom on the host framework. Moreover, as seen from Figs. 4(b) and 4(c), the $Au_{2,3,5,7,9}C^-$ clusters are more stable than the nearest clusters. These more stable structures are of 3D configuration (but 2D for the Au_2C^- cluster), and the C atom is saturated with coordination numbers of four, except for $Au_{2,3}C^-$ clusters.

C. Electronic properties

The electronic properties of Au_nC^- and Au_{n+1}^- ($n = 1-10$) clusters can be described by using the energy gap between the HOMO and LUMO, which reflects the ability for electrons to jump from an occupied orbital to an unoccupied orbital, as well as the ability for the molecule to participate in chemical reactions to some extent. A large value corresponds to an enhanced chemical stability. The HOMO and LUMO energies and the energy gaps for the lowest-energy Au_nC^- and Au_{n+1}^- ($n = 1-10$) clusters are listed in Table IV, with the corresponding curves shown in Fig. 5. As seen from Fig. 5, we can gain some important information about the most stable Au_nC^- and Au_{n+1}^- ($n = 1-10$) clusters. (a) The HOMO-LUMO gaps for the most stable Au_nC^- ($n = 1-10$) clusters range from 1.58 to 3.15 eV, where Au_3C^- and Au_4C^- clusters have the largest and smallest gap values, respectively. As for Au_{n+1}^- ($n = 1-10$) clusters, the HOMO-LUMO gaps range from 1.20 to 3.42 eV, where the gap value of Au_3^- is the largest and that of Au_8^- is the smallest. Additionally, the Au_{10}^- cluster has a nearly identical gap value (1.21 eV) with the Au_8^- cluster. By comparing the energy gaps of Au_nC^- and Au_{n+1}^- ($n = 1-10$) clusters, we can see that both of them show the same odd-even alternation phenomenon except for the Au_1C^- cluster. (b) It is well known that the doping of an impurity atom can increase or decrease the energy gap depending on its interaction with the host cluster. In the present

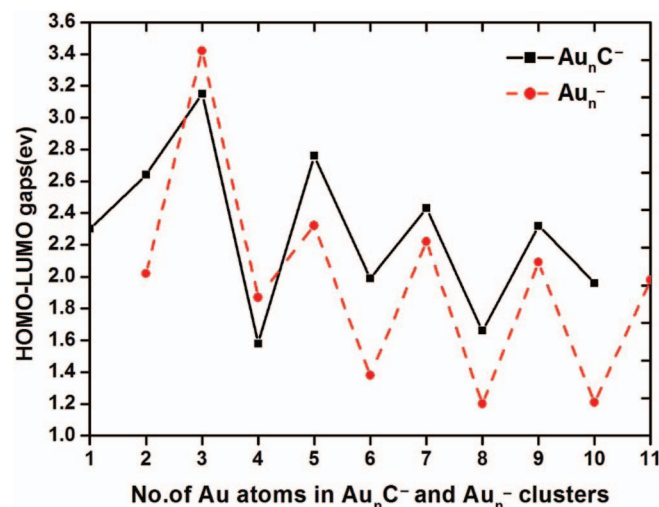


FIG. 5. Size dependence of the HOMO-LUMO gaps for the lowest-energy structure of Au_nC^- and Au_{n+1}^- ($n = 1-10$) clusters.

work, we can see that the interaction of C with Au_n^- clusters enlarges the energy gaps, except for Au_3^- and Au_4^- clusters. In other words, the doped C atom can enhance the chemical stability of pure gold clusters. In particular, the gap difference between Au_{10}^- and $Au_{10}C^-$ clusters is the largest (0.75 eV), which suggests that the $Au_{10}C^-$ cluster has skipping-increase chemical stability.

In light of the unusual phenomenon where the gaps of Au_3C^- and Au_4C^- clusters are less than those of Au_3^- and Au_4^- clusters, respectively, the eigenvalues of molecular frontier orbitals for these clusters are displayed in Fig. 6. Ten frontier orbitals are chosen for each kind of clusters. According to Fig. 6(a), we can see that both Au_3^- and Au_3C^- clusters are obviously characteristic of the degeneration of energy level nearby the HOMO and LUMO. Because of the incorporation of the C atom, the energy levels of the HOMO and LUMO are partially increased by 0.5 eV and 0.22 eV, respectively, thus leading to a net decrease in the energy gap of ~ 0.28 eV. Although the eigenvalues of the frontier orbitals in the Au_4^- and Au_4C^- clusters (see Fig. 6(b)) are very close, the energy levels are not degenerate. Furthermore, the participation of the C atom also increases the energy levels of the HOMO and LUMO by 0.49 eV and 0.19 eV, respectively, which results in a slight net decrease in the energy gap of ~ 0.3 eV. Generally, the incorporation of the C atom improves the energy levels of the HOMO and LUMO for Au_3^-

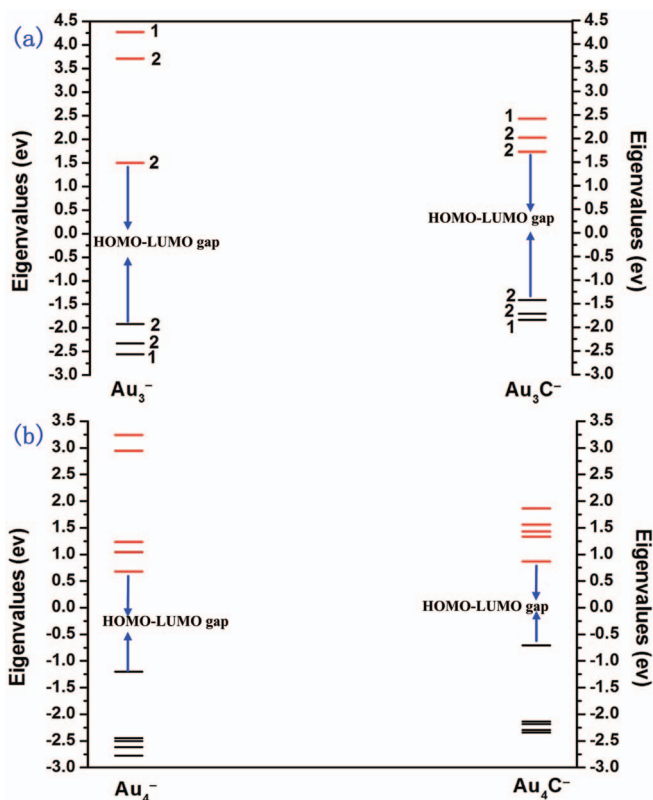


FIG. 6. Calculated molecular orbital eigenvalue spectra of Au_3^- and Au_3C^- clusters (a) along with Au_4^- and Au_4C^- clusters (b). The black lines represent the occupied orbitals and the red lines represent the unoccupied orbitals. The numbers beside the black and red lines indicate the degeneracy of the corresponding energy level. There is no degeneration in Au_4^- and Au_4C^- clusters, thus the degeneracy of the corresponding energy level is not labeled here. Ten frontier orbitals are chosen for each type of cluster.

TABLE V. Natural population analysis (NPA) and natural electron configuration (NEC) of C atoms in the lowest-energy Au_nC^- ($n = 1-10$) clusters at the PBE0/6-311G level of theory.

Cluster size	NPA ^a	NEC ^a
$n = 1$	-0.63944	$2s^{1.87}2p^{2.75}3s^{0.01}3p^{0.01}$
$n = 2$	-0.58538	$2s^{1.83}2p^{2.74}3p^{0.01}$
$n = 3$	-0.74767	$2s^{1.76}2p^{2.97}3p^{0.02}$
$n = 4$	-1.10410	$2s^{1.60}2p^{3.48}3s^{0.01}3p^{0.02}$
$n = 5$	-1.08152	$2s^{1.50}2p^{3.55}3s^{0.01}3p^{0.02}$
$n = 6$	-0.87305	$2s^{1.54}2p^{3.32}3p^{0.02}$
$n = 7$	-1.21437	$2s^{1.45}2p^{3.74}3s^{0.01}3p^{0.01}4p^{0.01}$
$n = 8$	-0.84950	$2s^{1.53}2p^{3.30}3s^{0.01}3p^{0.02}$
$n = 9$	-1.19460	$2s^{1.44}2p^{3.73}3s^{0.01}3p^{0.01}4p^{0.01}$
$n = 10$	-1.02550	$2s^{1.44}2p^{3.56}3p^{0.03}$

^aNPA and NEC are obtained from the NBO analysis in GAUSSIAN 09.

and Au_4^- clusters, but decreases the corresponding HOMO-LUMO gaps.

In the present work, it must be mentioned that various energy parameters in Fig. 4 are based on the total energy values of clusters and reflect the total thermodynamic stability. However, the HOMO-LUMO energy gap of a given cluster accurately lies on the eigenvalues of the HOMO and LUMO, which reflects its chemical stability. The VDE is the energy required to remove an extra electron from the anion by means of photoelectron spectroscopy, i.e., the energy difference between the HOMO and infinity. Therefore, all of them need not correlate directly with each other.^{41, 100}

It is well known that the NPA can provide a reasonable explanation for the localization of natural charge in clusters. To study the electronic properties, we have summarized the natural atomic charge population of C atom in the lowest-energy Au_nC^- ($n = 1-10$) clusters in Table V. As shown in Table V, the atomic charges of C atom are negative, indicating that the charges in the corresponding clusters transfer from the Au_n^- host to the C atom owing to the larger electronegativity of C than that of Au. Focusing on all the clusters, we can see that the charge-transfer values between Au_n^- host and C atom are less than an electron, except for Au_4C^- , Au_5C^- , Au_7C^- , Au_9C^- , and Au_{10}C^- clusters. Moreover, we also calculated the average ionic character of Au-C bonds for each kind of clusters based on the NBO analysis in GAUSSIAN 09, and the ionicity of the Au-C bond defined as follows:

$$i_{\text{Au,C}} = \left| \frac{C_{\text{Au}}^2 - C_{\text{C}}^2}{C_{\text{Au}}^2 + C_{\text{C}}^2} \right|, \quad (8)$$

where C_{Au}^2 and C_{C}^2 denote the polarization coefficients of Au and C atoms, respectively. The average ionicities of Au-C bonds in Au_4C^- , Au_5C^- , Au_7C^- , Au_9C^- , and Au_{10}C^- clusters are 28.49%, 25.78%, 27.81%, 27.91%, and 34.14%, respectively, all of which are less than 50%. Therefore, Au and C atoms interact with each other mainly through covalent bond rather than ionic bond, which can also be verified through the difference in electronegativity, Δ_{EN} . Covalently bonded interactions will exist in clusters if $\Delta_{\text{EN}} < 1.7$, and $\Delta_{\text{EN}} = 0.15$ for Au_nC^- clusters. Moreover, in order to further understand the above phenomenon, the internal charge transfer of the C atom is also taken into account by natu-

ral electronic configuration (NEC), which is also shown in Table V. With regard to the free C atom, the configuration of valence electrons is $2s^22p^2$. When the C atom is doped into gold clusters, the NEC analysis reveals that the $2s$ orbital loses 0.13–0.56 electrons, while the $2p$ orbital receives 0.74–1.74 electrons. In short, the charges mainly transfer between the $2s$ and $2p$ orbitals, and the effects of $3s$ and $3p$ orbitals can be neglected within the C atom.

IV. CONCLUSIONS

The geometrical structures, relative stabilities, and electronic properties of Au_nC^- and Au_{n+1}^- clusters have been investigated using hyper-GGA in PBE0 functional form, including the spin-orbit coupling effects (aiming at considering the relativistic effect). All of the results are summarized as follows:

1. The optimized geometries show that one Au atom capped on $\text{Au}_{n-1}\text{C}^-$ clusters is a dominant growth pattern for Au_nC^- clusters. The lowest-energy structures of Au_{n+1}^- clusters are planar, at least up to $n = 10$. The equilibrium geometries of C-doped Au clusters favor 3D configuration for $n = 3, 4, 5, 7, 9$; quasi-2D configuration for $n = 6, 8, 10$; and, as expected, 1D for Au_1C^- and 2D for Au_2C^- cluster. According to the ground-state geometries of Au_nC^- ($n = 3-10$) clusters, we can see that C doping induces local non-planarity while the remainder of the structure continues to grow on a planar mode, which results in an overall quasi-2D or 3D configuration. Thus, the C atom can dramatically alter the ground-state geometries of Au_n^- ($n = 1-10$) clusters.
2. The global minimum of the Au_4C^- cluster is not perfectly established because of the lack of experimental validation. In addition, the different performances of X in the corresponding Au_4X^- and Au_{16}X^- ($X = \text{C}, \text{Si}, \text{Ge}, \text{and Sn}$) clusters may be related to the extent of sp^3 hybridization and the Au-X bonding energy, etc., which deserves to be investigated further in terms of both theory and experimentation.
3. The higher atomic binding energies of Au_nC^- over Au_{n+1}^- ($n = 1-10$) clusters, along with the higher C atom attachment energy over Au attachment energy, reflect that the impurity C atom can significantly enhance the thermodynamic stability of pure gold clusters. Moreover, the convergent tendency of the average atomic binding energies for Au_nC^- and Au_{n+1}^- clusters suggests that the effect of the C atom on the Au_n^- host decreases with the increase of cluster size. Additionally, Figs. 4(b) and 4(c) show that the $\text{Au}_{2,3,5,7,9}\text{C}^-$ clusters are very stable clusters.
4. The electronic properties of Au_nC^- ($n = 1-10$) clusters are discussed based on the HOMO-LUMO energy gaps and the NBO analysis. The HOMO-LUMO gap curves show that the interaction of the C atom with Au_n^- clusters improves the chemical stability of pure gold clusters, except for Au_3^- and Au_4^- clusters. Furthermore, the NPA shows that the charges in corresponding Au_nC^-

clusters transfer from Au_n^- host to the C atom. Meanwhile, the NEC analysis also shows that the charges mainly transfer between the $2s$ and $2p$ orbitals within the C atom.

ACKNOWLEDGMENTS

The theoretical work was supported by the National Natural Science Foundation of China (NNSFC) (Grant No. 21073196), the State Key Program of National Natural Science of China (Grant No. 21133008), Director Foundation of AIOFM (Y23H161131 and Y03AG31146), and the Chinese Academy of Sciences. Acknowledgement is also made to the Thousand Youth Talents Plan. Part of computation was performed at Supercomputing Center of the Chinese Academy of Sciences and Supercomputing Center of USTC.

- ¹M. Haruta, *Catal. Today* **36**, 153 (1997).
- ²A. S. K. Hashmi and G. J. Hutchings, *Angew. Chem., Int. Ed.* **45**, 7896 (2006).
- ³B. M. Trost, *Angew. Chem., Int. Ed.* **34**, 259 (1995).
- ⁴G. C. Bond and D. T. Thompson, *Catal. Rev.* **41**, 319 (1999).
- ⁵G. J. Hutchings, *Catal. Today* **100**, 55 (2005).
- ⁶G. Bond, *Gold Bull.* **41**, 235 (2008).
- ⁷J. Das, M. A. Aziz, and H. Yang, *J. Am. Chem. Soc.* **128**, 16022 (2006).
- ⁸A. Corma and H. Garcia, *Chem. Soc. Rev.* **37**, 2096 (2008).
- ⁹L. S. Ott and R. G. Finke, *Coord. Chem. Rev.* **251**, 1075 (2007).
- ¹⁰J. D. Aiken III and R. G. Finke, *J. Mol. Catal. A: Chem.* **145**, 1 (1999).
- ¹¹F. Furche, R. Ahlrichs, P. Weis, C. Jacob, S. Gilb, T. Bierweiler, and M. M. Kappes, *J. Chem. Phys.* **117**, 6982 (2002).
- ¹²H. Häkkinen, B. Yoon, U. Landman, X. Li, H. J. Zhai, and L. S. Wang, *J. Phys. Chem. A* **107**, 6168 (2003).
- ¹³H. Häkkinen, M. Moseler, and U. Landman, *Phys. Rev. Lett.* **89**, 033401 (2002).
- ¹⁴W. Huang and L. S. Wang, *Phys. Rev. Lett.* **102**, 153401 (2009).
- ¹⁵X. Xing, B. Yoon, U. Landman, and J. H. Parks, *Phys. Rev. B* **74**, 165423 (2006).
- ¹⁶S. Bulusu, X. Li, L. S. Wang, and X. C. Zeng, *Proc. Natl. Acad. Sci. U.S.A.* **103**, 8326 (2006).
- ¹⁷J. Li, X. Li, H. J. Zhai, and L. S. Wang, *Science* **299**, 864 (2003).
- ¹⁸S. Bulusu, X. Li, L. S. Wang, and X. C. Zeng, *J. Phys. Chem. C* **111**, 4190 (2007).
- ¹⁹B. Yoon, P. Koskinen, B. Huber, O. Kostko, B. von Issendorff, H. Häkkinen, M. Moseler, and U. Landman, *Chem. Phys. Chem.* **8**, 157 (2007).
- ²⁰N. Shao, W. Huang, Y. Gao, L. M. Wang, X. Li, L. S. Wang, and X. C. Zeng, *J. Am. Chem. Soc.* **132**, 6596 (2010).
- ²¹A. Lechtken, D. Schooss, J. R. Stairs, M. N. Blom, F. Furche, N. Morgner, O. Kostko, B. von Issendorff, and M. M. Kappes, *Angew. Chem., Int. Ed.* **46**, 2944 (2007).
- ²²M. Ji, X. Gu, X. Li, X. Gong, J. Li, and L. S. Wang, *Angew. Chem.* **117**, 7281 (2005).
- ²³J. P. Doye and D. J. Wales, *New J. Chem.* **22**, 733 (1998).
- ²⁴W. Huang, M. Ji, C. D. Dong, X. Gu, L. M. Wang, X. G. Gong, and L. S. Wang, *ACS Nano* **2**, 897 (2008).
- ²⁵K. Michaelian, N. Rendon, and I. Garzón, *Phys. Rev. B* **60**, 2000 (1999).
- ²⁶I. Garzón, K. Michaelian, M. Beltrán, A. Posada-Amarillas, P. Ordejón, E. Artacho, D. Sánchez-Portal, and J. Soler, *Phys. Rev. Lett.* **81**, 1600 (1998).
- ²⁷L. M. Wang and L. S. Wang, *Nanoscale* **4**, 4038 (2012).
- ²⁸G. Jian-Jun, Y. Ji-Xian, and D. Dong, *Physica B* **367**, 158 (2005).
- ²⁹G. Jian-Jun, Y. Ji-Xian, and D. Dong, *J. Mol. Struct.: THEOCHEM* **764**, 117 (2006).
- ³⁰S. J. Wang, X. Y. Kuang, C. Lu, Y. F. Li, and Y. R. Zhao, *Phys. Chem. Chem. Phys.* **13**, 10119 (2011).
- ³¹Y. Li, Y. P. Cao, Y. F. Li, S. P. Shi, and X. Y. Kuang, *Eur. Phys. J. D* **66**, 10 (2012).
- ³²L. M. Wang, R. Pal, W. Huang, X. C. Zeng, and L. S. Wang, *J. Chem. Phys.* **132**, 114306 (2010).
- ³³D. Yuan, Y. Wang, and Z. Zeng, *J. Chem. Phys.* **122**, 114310 (2005).
- ³⁴D. Dong, K. Xiao-Yu, Z. Bing, and G. Jian-Jun, *Physica B* **406**, 3160 (2011).
- ³⁵D. Dong, K. Xiao-Yu, G. Jian-Jun, and Z. Ben-Xia, *J. Phys. Chem. Solids* **71**, 770 (2010).
- ³⁶D. Dong, Z. Ben-Xia, and Z. Bing, *Mol. Phys.* **109**, 1709 (2011).
- ³⁷H. Q. Wang, X. Y. Kuang, and H. F. Li, *J. Phys. Chem. A* **113**, 14022 (2009).
- ³⁸C. Majumder, A. K. Kandalam, and P. Jena, *Phys. Rev. B* **74**, 205437 (2006).
- ³⁹C. Rajesh and C. Majumder, *J. Chem. Phys.* **130**, 234309 (2009).
- ⁴⁰C. Majumder, *Phys. Rev. B* **75**, 235409 (2007).
- ⁴¹C. Majumder and S. Kulshreshtha, *Phys. Rev. B* **73**, 155427 (2006).
- ⁴²M. Zhang, S. Chen, Q. M. Deng, L. M. He, L. N. Zhao, and Y. H. Luo, *Eur. Phys. J. D* **58**, 117 (2010).
- ⁴³B. Kiran, X. Li, H. J. Zhai, L. F. Cui, and L. S. Wang, *Angew. Chem.* **116**, 2177 (2004).
- ⁴⁴C. Pak, J. C. Rienstra-Kiracofe, and H. F. Schaefer, *J. Phys. Chem. A* **104**, 11232 (2000).
- ⁴⁵B. Kiran, X. Li, H.-J. Zhai, and L.-S. Wang, *J. Chem. Phys.* **125**, 133204 (2006).
- ⁴⁶X. Li, B. Kiran, and L. S. Wang, *J. Phys. Chem. A* **109**, 4366 (2005).
- ⁴⁷R. Pal, S. Bulusu, and X. C. Zeng, *J. Comput. Methods Sci. Eng.* **7**, 185 (2007).
- ⁴⁸L. M. Wang, S. Bulusu, W. Huang, R. Pal, L. S. Wang, and X. C. Zeng, *J. Am. Chem. Soc.* **129**, 15136 (2007).
- ⁴⁹Q. Sun, Q. Wang, G. Chen, and P. Jena, *J. Chem. Phys.* **127**, 214706 (2007).
- ⁵⁰W. Fa and A. Yang, *Phys. Lett. A* **372**, 6392 (2008).
- ⁵¹D. Balamurugan, M. K. Harbola, and R. Prasad, *Phys. Rev. A* **69**, 033201 (2004).
- ⁵²B. R. Visser, M. A. Addicoat, J. R. Gascooke, W. D. Lawrance, and G. F. Metha, *J. Chem. Phys.* **138**, 174310 (2013).
- ⁵³B. W. Ticknor, B. Bandyopadhyay, and M. A. Duncan, *J. Phys. Chem. A* **112**, 12355 (2008).
- ⁵⁴P. Zaleski-Ejgierd and P. Pyykkö, *Can. J. Chem.* **87**, 798 (2009).
- ⁵⁵D. Z. Li and S. D. Li, *J. Cluster Sci.* **22**, 331 (2011).
- ⁵⁶X. Y. Sun, J. G. Du, and G. Jiang, *Struct. Chem.* **24**, 1289 (2013).
- ⁵⁷M. Barysz and P. Pyykkö, *Chem. Phys. Lett.* **285**, 398 (1998).
- ⁵⁸P. Pyykkö, M. Patzschke, and J. Suurpere, *Chem. Phys. Lett.* **381**, 45 (2003).
- ⁵⁹M. Iwamatsu and Y. Okabe, *Chem. Phys. Lett.* **399**, 396 (2004).
- ⁶⁰H. G. Kim, S. K. Choi, and H. M. Lee, *J. Chem. Phys.* **128**, 144702 (2008).
- ⁶¹D. J. Wales and J. P. Doye, *J. Chem. Phys. A* **101**, 5111 (1997).
- ⁶²B. Delley, *J. Chem. Phys.* **92**, 508 (1990).
- ⁶³R. A. Kendall, E. Aprà, D. E. Bernholdt, E. J. Bylaska, M. Dupuis, G. I. Fann, R. J. Harrison, J. Ju, J. A. Nichols, and J. Nieplocha, *Comput. Phys. Commun.* **128**, 260 (2000).
- ⁶⁴M. J. Frisch, G. W. Trucks, H. B. Schlegel *et al.*, GAUSSIAN 09, Revision A.02, Gaussian, Inc., Wallingford, CT, 2009.
- ⁶⁵P. Schwerdtfeger, *Heteroat. Chem.* **13**, 578 (2002).
- ⁶⁶P. Schwerdtfeger, M. Dolg, W. E. Schwarz, G. A. Bowmaker, and P. D. Boyd, *J. Chem. Phys.* **91**, 1762 (1989).
- ⁶⁷P. Schwerdtfeger, *J. Am. Chem. Soc.* **111**, 7261 (1989).
- ⁶⁸P. Schwerdtfeger, P. D. Boyd, A. K. Burrell, W. T. Robinson, and M. J. Taylor, *Inorg. Chem.* **29**, 3593 (1990).
- ⁶⁹P. Schwerdtfeger, P. D. Boyd, S. Brienne, and A. K. Burrell, *Inorg. Chem.* **31**, 3411 (1992).
- ⁷⁰P. Schwerdtfeger and G. A. Bowmaker, *J. Chem. Phys.* **100**, 4487 (1994).
- ⁷¹R. Wesendrup, J. K. Laerdahl, and P. Schwerdtfeger, *J. Chem. Phys.* **110**, 9457 (1999).
- ⁷²N. Werthamer, E. Helfand, and P. Hohenberg, *Phys. Rev.* **147**, 295 (1966).
- ⁷³G. Satchler, *Nucl. Phys.* **55**, 1 (1964).
- ⁷⁴G. Dresselhaus, *Phys. Rev.* **100**, 580 (1955).
- ⁷⁵R. Pal, L. M. Wang, W. Huang, L. S. Wang, and X. C. Zeng, *J. Chem. Phys.* **134**, 054306 (2011).
- ⁷⁶Y. L. Wang, H. J. Zhai, L. Xu, J. Li, and L. S. Wang, *J. Phys. Chem. A* **114**, 1247 (2010).
- ⁷⁷W. Huang, S. Bulusu, R. Pal, X. C. Zeng, and L. S. Wang, *ACS Nano* **3**, 1225 (2009).
- ⁷⁸W. Huang, R. Pal, L. M. Wang, X. C. Zeng, and L. S. Wang, *J. Chem. Phys.* **132**, 054305 (2010).

- ⁷⁹R. Pal, W. Huang, Y. L. Wang, H. S. Hu, S. Bulusu, X. G. Xiong, J. Li, L. S. Wang, and X. C. Zeng, *J. Phys. Chem. Lett.* **2**, 2288 (2011).
- ⁸⁰W. Huang, S. Bulusu, R. Pal, X. C. Zeng, and L. S. Wang, *J. Chem. Phys.* **131**, 234305 (2009).
- ⁸¹A. E. Reed, L. A. Curtiss, and F. Weinhold, *Chem. Rev.* **88**, 899 (1988).
- ⁸²A. E. Reed and F. Weinhold, *J. Chem. Phys.* **78**, 4066 (1983).
- ⁸³C. Hättig, D. P. Tew, and A. Köhn, *J. Chem. Phys.* **132**, 231102 (2010).
- ⁸⁴T. B. Adler, G. Knizia, and H. J. Werner, *J. Chem. Phys.* **127**, 221106 (2007).
- ⁸⁵G. Knizia, T. B. Adler, and H. J. Werner, *J. Chem. Phys.* **130**, 054104 (2009).
- ⁸⁶D. P. Tew and W. Klopper, *Mol. Phys.* **108**, 315 (2010).
- ⁸⁷H. J. Werner, P. J. Knowles, G. Knizia, F. R. Manby, and M. Schütz, *WIREs Comput. Mol. Sci.* **2**, 242 (2012).
- ⁸⁸See supplementary material at <http://dx.doi.org/10.1063/1.4852179> for more information on top-several low-lying structures of Au_n^- ($n = 2-11$) clusters, structural parameters of the lowest-energy Au_nC^- ($n = 1-10$) clusters, main methods, basis sets, and software packages used for optimization and single-point energy calculations, and simulated photoelectron spectra of Au_nC^- ($n = 1-10$) clusters.
- ⁸⁹F. Remacle and E. Kryachko, *J. Chem. Phys.* **122**, 044304 (2005).
- ⁹⁰H. Häkkinen and U. Landman, *Phys. Rev. B* **62**, R2287 (2000).
- ⁹¹K. Taylor, C. Pettiette-Hall, O. Cheshnovsky, and R. Smalley, *J. Chem. Phys.* **96**, 3319 (1992).
- ⁹²S. K. Sahoo, S. Nigam, P. Sarkar, and C. Majumder, *Chem. Phys. Lett.* **543**, 121 (2012).
- ⁹³F. Y. Naumkin, *Comput. Theor. Chem.* **1021**, 191 (2013).
- ⁹⁴R. Pal, L. M. Wang, W. Huang, L. S. Wang, and X. C. Zeng, *J. Am. Chem. Soc.* **131**, 3396 (2009).
- ⁹⁵J. Ho, K. M. Ervin, and W. Lineberger, *J. Chem. Phys.* **93**, 6987 (1990).
- ⁹⁶I. Mayer, *Chem. Phys. Lett.* **97**, 270 (1983).
- ⁹⁷K. B. Wiberg, *Tetrahedron* **24**, 1083 (1968).
- ⁹⁸I. Mayer, *Int. J. Quantum Chem.* **29**, 477 (1986).
- ⁹⁹I. Mayer, *Theor. Chim. Acta* **67**, 315 (1985).
- ¹⁰⁰C. Majumder and S. Kulshreshtha, *Phys. Rev. B* **69**, 075419 (2004).